

Effect of electron-doping on spin excitations of underdoped $\text{BaFe}_{1.96}\text{Ni}_{0.04}\text{As}_2$

Leland W. Harriger,¹ Astrid Schneidewind,² Shiliang Li,^{1,3} Jun Zhao,¹ Zhengcai Li,³ Wei Lu,³ Xiaoli Dong,³ Fang Zhou,³ Zhongxian Zhao,³ Jiangping Hu,⁴ and Pengcheng Dai^{1,3,5,*}

¹ *Department of Physics and Astronomy, The University of Tennessee, Knoxville, Tennessee 37996-1200, USA*

² *Technische Universität Dresden, Institut für Festkörperphysik, 01062 Dresden, Germany*

³ *Institute of Physics, Chinese Academy of Sciences, Beijing 100080, China*

⁴ *Department of Physics, Purdue University, West Lafayette, IN 47907*

⁵ *Neutron Scattering Science Division, Oak Ridge National Laboratory, Oak Ridge, Tennessee 37831-6393, USA*

We use neutron scattering to study magnetic order and spin excitations in $\text{BaFe}_{1.96}\text{Ni}_{0.04}\text{As}_2$. On cooling, the system first changes the lattice symmetry from tetragonal to orthorhombic near ~ 97 K, and then orders antiferromagnetically at $T_N = 91$ K before developing weak superconductivity below ~ 15 K. Although superconductivity appears to co-exist with static antiferromagnetic order from transport and neutron diffraction measurement, inelastic neutron scattering experiments reveal that magnetic excitations do not respond to superconductivity. Instead, the effect of electron-doping is to reduce the c -axis exchange coupling in BaFe_2As_2 and induce quasi two-dimensional spin excitations. These results suggest that transition from three-dimensional spin waves to two-dimensional spin excitations by electron-doping is important for the separated structural/magnetic phase transitions and high-temperature superconductivity in iron arsenides.

PACS numbers: 74.25.Ha, 74.70.-b, 78.70.Nx

Antiferromagnetism is relevant to high temperature (high- T_c) superconductivity in copper oxides and iron arsenides because superconductivity arises from electron- or hole-doping of their static antiferromagnetic (AF) ordered parent compounds [1, 2, 3, 4, 5, 6, 7, 8, 9]. In the case of cuprates, spin waves of the parent materials can be very well described by a local moment Heisenberg Hamiltonian and spin excitations in optimally doped superconductors are dominated by a neutron spin resonance centered at the AF ordering wavevector [1, 2, 3]. For undoped iron arsenides such as $A\text{Fe}_2\text{As}_2$ ($A = \text{Ba}, \text{Sr}, \text{Ca}$) with a spin structure of Fig. 1a [10], spin waves consist of a large anisotropy gap at the AF zone center [$\Delta(1, 0, 1) \leq 9.8$ meV] and excitations extend up to ~ 200 meV [11, 12, 13, 14, 15]. For optimally doped superconductors [5, 6, 7], the gapped spin wave excitations were replaced by a gapless continuum of scattering in the normal state and a neutron spin resonance below T_c [16, 17, 18, 19]. Since spin fluctuations may play a crucial role in the electron pairing and superconductivity of iron arsenides [20, 21, 22, 23, 24, 25, 26, 27], it is imperative to determine how the spin dynamics of the undoped AF parent compounds evolve as they are tuned toward optimally doped superconductivity by electron or hole doping.

In the undoped state, BaFe_2As_2 exhibits simultaneous structural and magnetic phase transitions below $T_s = T_N = 143$ K, changing the crystal lattice symmetry from the high-temperature tetragonal to low-temperature orthorhombic phase [10]. Upon Co-doping to induce electrons onto the FeAs plane, the combined AF and structural phase transitions were split into two distinct transitions and the electronic phase diagram in the lower Co-doping region displays coexisting static AF order with

the superconductivity [28, 29]. Although recent neutron scattering experiments confirmed that the upper transition is structural and the AF order occurs at lower temperature [30, 31, 32], its microscopic origin is still unknown. More importantly, it is unclear what happens to the spin waves of BaFe_2As_2 when electrons are doped into these materials. While Pratt *et al.* [30] reported gapless normal state spin excitations for $\text{BaFe}_{1.906}\text{Co}_{0.094}\text{As}_2$, measurements on $\text{BaFe}_{1.92}\text{Co}_{0.08}\text{As}_2$ suggest gapped normal state excitations [32]. On cooling below T_c , both materials reveal a reduction in the static ordered AF moment and the appearance of a spin resonance [30, 32].

To compare with the results obtained on Co-doped BaFe_2As_2 [28, 29, 30, 31, 32], we carried out neutron scattering experiments on Ni-doped $\text{BaFe}_{1.96}\text{Ni}_{0.04}\text{As}_2$ ($T_c \approx 15$ K, Figs. 1c,1d) [7]. In contrast to the results on Co-doped materials [30, 32], we find that the static AF order and spin excitations in $\text{BaFe}_{1.96}\text{Ni}_{0.04}\text{As}_2$ do not respond to the occurrence of superconductivity. Instead, the effect of electron-doping is to significantly reduce the c -axis exchange coupling and change the three-dimensional (3D) spin waves of BaFe_2As_2 into quasi two-dimensional (2D). These results suggest that the separated structural/magnetic phase transition and the appearance of bulk superconductivity upon doping may be associated with the diminishing spin anisotropy gap and the 3D to 2D transition of the spin excitations.

Using the self-flux method [7], we grew a ~ 1 gram single crystal of $\text{BaFe}_{1.96}\text{Ni}_{0.04}\text{As}_2$ with an in-plane and out-of-plane mosaic of 1.74° and 2.20° full-width at half maximum (FWHM), respectively. We defined the wave vector Q at (q_x, q_y, q_z) as $(H, K, L) = (q_x a / 2\pi, q_y b / 2\pi, q_z c / 2\pi)$ reciprocal lattice units (rlu) using the orthorhombic magnetic unit cell (space group Fmmm), where $a = 5.5 \text{ \AA}$,

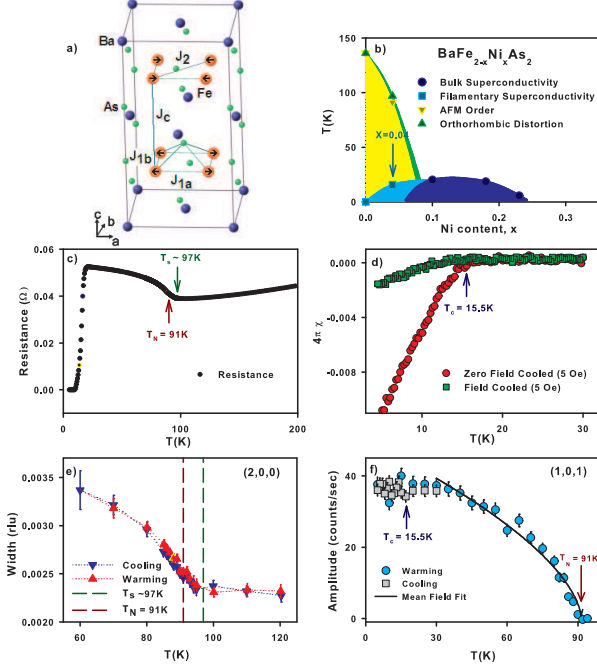


FIG. 1: (color online). (a) Diagram of the parent compound BaFe_2As_2 with Fe spin ordering and magnetic exchange couplings depicted. We use the same unit cell for $\text{BaFe}_{1.96}\text{Ni}_{0.04}\text{As}_2$. (b) Electronic phase diagram from Ref. [7]. (c) Temperature dependence of the resistance showing anomalies at T_s , T_N , and T_c . (d) Temperature dependence of the Meissner and shielding signals on a small crystal (field cooled $4\pi\chi = -0.001$ at 4.5 K). (e) Temperature dependence of the structural distortion of the lattice as determined by tracking the width of the $(2,0,0)$ nuclear Bragg peak using $\lambda/2$ scattering without Be filter. (f) Magnetic order parameter determined by Q -scans around $(1,0,1)$ magnetic Bragg peak above background. The solid line shows order parameter fit using $\phi^2 \propto (1 - T/T_N)^{2\beta}$ with $T_N = 91.3 \pm 0.7$ K and $\beta = 0.3 \pm 0.02$.

$b = 5.4 \text{ \AA}$, and $c = 12.77 \text{ \AA}$. We performed our neutron scattering experiment on the PANDA cold triple-axis spectrometer at the Forschungsneutronenquelle Heinz Maier-Leibnitz (FRM II), TU Munchen, Germany as described earlier [18]. Our sample was aligned in the $[H, 0, L]$ zone inside a closed cycle refrigerator.

Figures 1c and 1d show the resistivity and susceptibility data. The resistivity shows clear anomalies near 97 K and 91 K before superconductivity sets in below ~ 15 K (Fig. 1c). Although the presence of superconductivity below $T_c \approx 15$ K is confirmed in the susceptibility measurement (Fig. 1d), the weak Meissner effect suggests superconducting volume fraction of less than 0.2%.

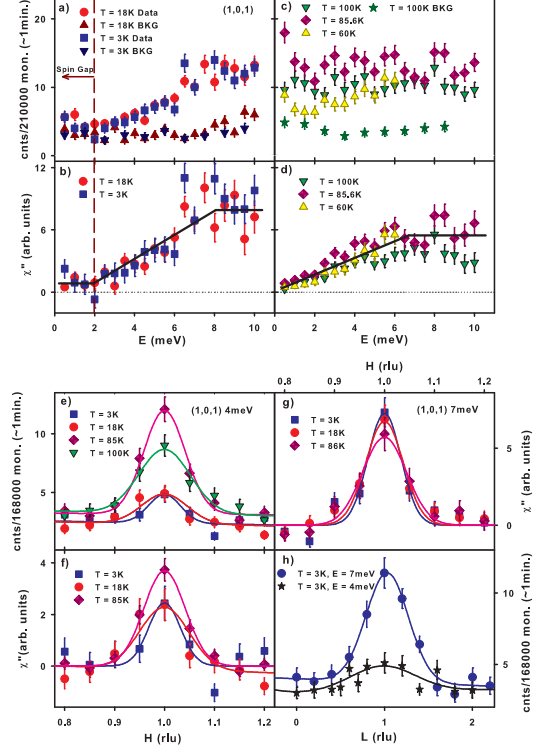


FIG. 2: (color online). (a) Energy scans at $Q = (1,0,1)$ and $Q = (1.2,0,1)$ above and below T_c . (b) $\chi''(Q,\omega)$ at $Q = (1,0,1)$. (c) Energy scans at higher temperatures and, (d) the corresponding $\chi''(Q,\omega)$. (e) Q -scans along the $[H, 0, 1]$ direction at 4 meV and different temperatures. Fourier transforms of the Gaussian peaks give minimum correlation lengths of $\xi = 57 \pm 4 \text{ \AA}$ (f) Estimated $\chi''(Q,\omega)$ at 4 meV. (g) $\chi''(Q,\omega)$ at 7 meV with minimum correlation length of $\xi = 54 \pm 6 \text{ \AA}$. (h) Low temperature Q -scans along the $[1, 0, L]$ direction (c -axis) at 4 meV and 7 meV. The minimum dynamic spin correlation lengths are $\xi \approx 14 \pm 5$ and $21 \pm 2 \text{ \AA}$ for 4 and 7 meV, respectively.

Similar to Co-doped BaFe_2As_2 [30, 31, 32], we find that the tetragonal to orthorhombic structural transition happens at 97 K while the AF order occurs below $T_N = 91$ K (Figs. 1e and 1f). However, in contrast with Co-doped materials [30, 32], superconductivity has no influence on the static AF order of $\text{BaFe}_{1.96}\text{Ni}_{0.04}\text{As}_2$ (Fig. 1f). This is consistent with the fact that our sample has a lower electron-doping to the FeAs-plane than those of Refs. [30, 32].

In the undoped BaFe_2As_2 , spin waves have an anisotropy gap about 8 meV at $Q = (1,0,1)$ [$\Delta(1,0,1) = 8 \text{ meV}$] [12, 14]. For optimally Co and Ni doped materials, spin excitations are gapless in the normal state [17, 18] and superconductivity-induced spin gaps open below T_c [19]. Figure 2a shows the constant- Q scans at the $Q = (1,0,1)$ (signal) and $Q = (1.2,0,1)$ (background)

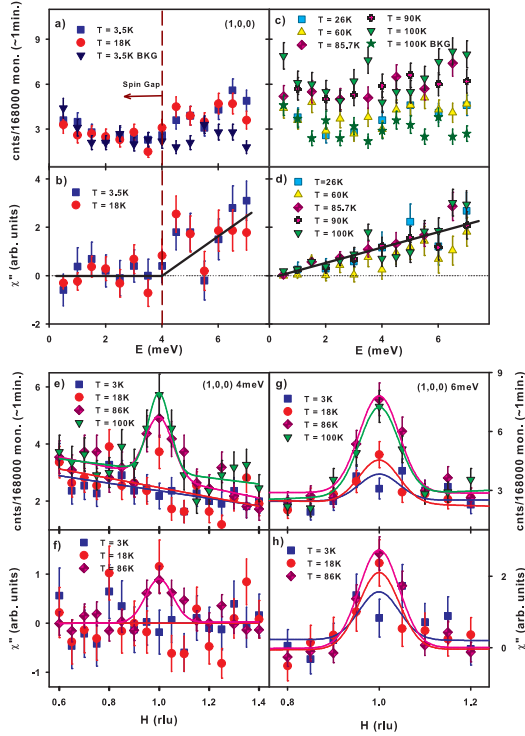


FIG. 3: (color online). (a) Energy scans at $Q = (1, 0, 0)$ and $Q = (1.4, 0, 0)$ from 0.5 meV to 7 meV at 3.5 K and 18 K. (b) Background corrected $\chi''(Q, \omega)$ showing clear evidence for a 4 meV spin gap, larger than that at $Q = (1, 0, 0)$. (c) Temperature dependence of the signal [$Q = (1, 0, 0)$] and background [$Q = (1.4, 0, 0)$] scattering at various temperatures. (d) $\chi''(Q, \omega)$ at 4 meV. (e) Q -scans along the $[H, 0, 0]$ direction at 4 meV and different temperatures. A peak centered at $Q = (1, 0, 0)$ appears above 80 K. (f) Background corrected $\chi''(Q, \omega)$. (g) Temperature dependence of the Q -scans along the $[H, 0, 0]$ direction at 6 meV. The scattering has a peak at 3 K. (h) Temperature dependence of the $\chi''(Q, \omega)$ at 6 meV.

positions above and below T_c for $\text{BaFe}_{1.96}\text{Ni}_{0.04}\text{As}_2$. Figure 2b plots the imaginary part of the dynamic susceptibility $\chi''(Q, \omega)$ after correcting for background and Bose population factor. We find that $\chi''(Q, \omega)$ has a 2 meV spin gap and is not affected by superconductivity. Figures 2c and 2d reveal that the magnetic intensity increase with increasing temperature below T_N is due mostly to the Bose population factor. These results are confirmed by Q -scans along the $[H, 0, 1]$ direction at different temperatures (Figs. 2e-2g), which display well-defined peaks at $Q = (1, 0, 1)$ that have similar widths to the undoped BaFe_2As_2 at 10 meV [14]. Figure 4h shows Q -scans along the c -axis $[1, 0, L]$ direction. In contrast to the in-plane spin excitations, the c -axis spin-spin correlations are much broader for $\text{BaFe}_{1.96}\text{Ni}_{0.04}\text{As}_2$, thus suggesting 2D nature of the excitations.

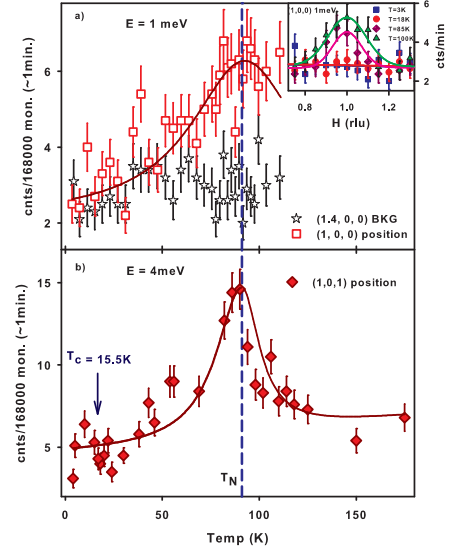


FIG. 4: (color online). (a) Temperature dependence of the 1 meV scattering at the signal $Q = (1, 0, 0)$ and background $Q = (1.4, 0, 0)$ positions. The inset shows Q -scans along the $[H, 0, 0]$ at 1 meV and different temperatures. The scattering shows no anomaly across T_c but clearly peak at T_N . (b) Temperature dependence of the scattering at 4 meV and $Q = (1, 0, 1)$ again peaks at T_N .

Further evidences for 2D spin excitations in $\text{BaFe}_{1.96}\text{Ni}_{0.04}\text{As}_2$ are summarized in Fig. 3. Assuming spin excitations in $\text{BaFe}_{2-x}\text{Ni}_x\text{As}_2$ can be described by an effective Heisenberg Hamiltonian, the spin anisotropy gaps at $Q = (1, 0, 1)$ and $Q = (1, 0, 0)$ are $\Delta(1, 0, 1) = 2S[(J_{1a} + 2J_2 + J_c + J_s)^2 - (J_c + J_{1a} + 2J_2)^2]^{1/2}$ and $\Delta(1, 0, 0) = 2S[(2J_{1a} + 4J_2 + J_s)(2J_c + J_s)]^{1/2}$, respectively [11, 12, 14, 15]. Here S is the magnetic spin ($= 1$); J_{1a} , J_2 , J_c , J_s are effective in-plane nearest-neighbor, next nearest-neighbor, c -axis, and magnetic single ion anisotropy couplings, respectively (Fig. 1a). For BaFe_2As_2 , we estimate $\Delta(1, 0, 1) = 7.8$ meV and $\Delta(1, 0, 0) = 20.2$ meV assuming $J_{1a} = 36$, $J_2 = 18$, $J_c = 0.3$, $J_s = 0.106$ meV [12, 14, 15]. Upon electron doping to form $\text{BaFe}_{1.96}\text{Ni}_{0.04}\text{As}_2$, these spin gap values have been reduced to $\Delta(1, 0, 1) = 2$ meV and $\Delta(1, 0, 0) = 4$ meV (Figs. 2b and 3b). Since such electron-doping hardly changes the in-plane Q -scan widths compared to that of the undoped BaFe_2As_2 (Figs. 2e-g, 3e, 3g) [12, 14], it should only slightly modify the in-plane exchange couplings. Assuming that J_{1a} and J_2 are unchanged in $\text{BaFe}_{1.96}\text{Ni}_{0.04}\text{As}_2$, the observed $\Delta(1, 0, 1) = 2$ meV and $\Delta(1, 0, 0) = 4$ meV would correspond to $J_c = 0.01$ meV and $J_s = 0.007$ meV, suggesting a rapid suppression of c -axis exchange coupling and magnetic single ion anisotropy with electron doping.

In Ref. [32], it was argued that spin anisotropy for

BaFe_{1.92}Co_{0.08}As₂ is similar to that of the BaFe₂As₂, meaning that the reduction in spin gap at $Q = (1, 0, 1)$ arises mostly from reduced J_{1a} and J_2 . Assuming the best fitted values of $S(J_{1a} + 2J_2) = 32$ meV and $SJ_c = 0.34$ meV [32], we expect $\Delta(1, 0, 1) = 5.5$ meV and $\Delta(1, 0, 0) = 14.2$ meV with $SJ_s = 0.106$ meV. These values are clearly different from the observation. Even if we assume all exchange couplings to reduce by 50% upon electron-doping with $S(J_{1a} + 2J_2) = 32$ meV, $SJ_c = 0.15$ meV, and $SJ_s = 0.05$ meV, we still find $\Delta(1, 0, 1) = 3.8$ and $\Delta(1, 0, 0) = 10$ meV. This suggests that the large reduction in the $\Delta(1, 0, 0)$ gap values upon electron doping is due to the reduced J_c and three-dimensionality of the system.

To determine the temperature dependence of $\Delta(1, 0, 0)$, we show in Fig. 3c the observed scattering at the signal $Q = (1, 0, 0)$ and background $(1.4, 0, 0)$ positions at several temperatures. Figure 3d plots the estimated $\chi''(Q, \omega)$. Comparing Fig. 3d with Fig. 3b, the 4 meV spin gap $\chi''(Q, \omega)$ at 18 K vanishes upon warming to above 60 K. These results are confirmed by Q -scans at 4 meV along the $[H, 0, 0]$ direction (Fig. 3e). While scans at 2 K and 18 K are featureless, the scattering at 86 K and 100 K shows clear peaks centered at $Q = (1, 0, 0)$. For Q -scans at 6 meV, the scattering shows well-defined peaks at all temperatures (Fig. 3g). Converting these data into $\chi''(Q, \omega)$ in Fig. 3h confirms the results of Fig. 3d.

Finally, we show in Fig. 4a the temperature dependence of the 1 meV scattering at the $Q = (1, 0, 0)$ (signal) and $Q = (1.4, 0, 0)$ (background) positions. While the background scattering only increases slightly with increasing temperature and shows no anomaly across T_N , the scattering at $Q = (1, 0, 0)$ clearly peaks at T_N . Q -scans along the $[H, 0, 0]$ direction at 1 meV confirm these results (the inset of Fig. 4a). Temperature dependence of the scattering at 4 meV and $Q = (1, 0, 1)$ show similar behavior (Fig. 4b). These results suggest that the disappearing $\Delta(1, 0, 1)$ and $\Delta(1, 0, 0)$ gaps near T_N arise from critical scattering associated with the static AF order.

To understand the separated structural and magnetic phase transitions for BaFe_{1.96}Ni_{0.04}As₂, we note that in an effective J_1 - J_2 - J_c model [22, 23], the separation of the lattice and magnetic transition temperatures is controlled by the value of J_c [22]. There is only one transition temperature when J_c is large. A finite separation between the two transition temperatures occurs when J_c/J_2 is reduced to the order of 10^{-3} . Our experimental result of $J_c/J_2 \sim 0.5 \times 10^{-3}$ is consistent with this picture. To quantitatively estimate the reduced T_N due to the smaller J_c , we note that $T_N \sim J_2/\ln(J_2/J_c)$ [22]. Let J_α^0 be the magnetic exchange values for the parental compounds, we can write $T_N^0/T_N = a[\ln(a) + \ln(b) + \ln(c)]/\ln(c)$, where $a = J_2^0/J_2$, $b = J_c^0/J_c$, $c = J_2^0/J_c^0$. Using the experimental values of the exchange coupling parameters determined earlier, we obtain $(J_2/J_2^0) = (1/a) \sim 0.87$,

which is self-consistent with our suggestion that upon doping, the coupling between layers J_c is dramatically reduced while the change of the in-plane magnetic exchange coupling is small. These results provide a natural and consistent interpretation for our experimental observations.

In summary, we have shown that the most dramatic effect of electron-doping in BaFe₂As₂ is to transform the 3D anisotropic spin waves into 2D spin excitations. These results suggest that reduced dimensionality in spin excitations of iron arsenides is important for the separated structural/magnetic phase transition and the occurrence of high- T_c superconductivity in these materials.

We thank C. Xu for helpful discussions. This work is supported by the U.S. NSF No. DMR-0756568, U.S. DOE BES No. DE-FG02-05ER46202, and by the U.S. DOE, Division of Scientific User Facilities. The work in IOP is supported by the Ministry of Science and Technology of China and NSFC. We further acknowledge support from DFG within Sonderforschungsbereich 463 and from the PANDA project of TU Dresden and FRM II.

* Electronic address: daip@ornl.gov

- [1] P. A. Lee, N. Nagaosa, and X.-G. Wen, Rev. Mod. Phys. **78**, 17 (2006).
- [2] R. J. Birgeneau *et al.*, J. Phys. Soc. Jpn. **75**, 111003 (2008).
- [3] E. Eschrig, Adv. Phys. **55**, 47 (2006).
- [4] Y. Kamihara *et al.*, J. Am. Chem. Soc. **130**, 3296 (2008).
- [5] M. Rotter *et al.*, Phys. Rev. Lett. **101**, 107006 (2008).
- [6] A. S. Sefat *et al.*, Phys. Rev. Lett. **101**, 117004 (2008).
- [7] L. J. Li *et al.*, New. J. Phys. **11**, 025008 (2009).
- [8] C. de la Cruz *et al.*, Nature (London) **453**, 899 (2008).
- [9] J. Zhao *et al.*, Nature Materials **7**, 953 (2008).
- [10] J. W. Lynn and Pengcheng Dai, arXiv:0902.0091.
- [11] J. Zhao *et al.*, Phys. Rev. Lett. **101**, 167203 (2008).
- [12] R. A. Ewings *et al.*, Phys. Rev. B **78**, 220501(R) (2008).
- [13] R. J. McQueeney *et al.*, Phys. Rev. Lett. **101**, 227205 (2008).
- [14] K. Matan *et al.*, Phys. Rev. B **79**, 054526 (2009).
- [15] J. Zhao *et al.*, arXiv: 0903.2686.
- [16] A. D. Christianson *et al.*, Nature (London) **456**, 930 (2008).
- [17] M. D. Lumsden *et al.*, Phys. Rev. Lett. **102**, 107005 (2009).
- [18] Songxue Chi *et al.*, Phys. Rev. Lett. **102**, 107006 (2009).
- [19] Shiliang Li *et al.*, arXiv: 0902.0813.
- [20] I. I. Mazin and J. Schmalian, arXiv:0901.4790.
- [21] J. Dai *et al.*, PNAS **106**, 4118 (2009).
- [22] C. Fang *et al.*, Phys. Rev. B **77**, 224509 (2008).
- [23] C. Xu *et al.*, Phys. Rev. B **78**, 020501(R) (2008).
- [24] K. Seo *et al.*, Phys. Rev. Lett. **101**, 206404 (2008).
- [25] F. Wang *et al.*, Phys. Rev. Lett. **102**, 047005 (2009).
- [26] Z. Y. Weng, arXiv:0804.3228.
- [27] A. V. Chubukov, arXiv:0902.4188.
- [28] N. Ni *et al.*, Phys. Rev. B **78**, 214515 (2008).
- [29] J.-H. Chu *et al.*, Phys. Rev. B **79**, 014506 (2008).

[30] D. K. Pratt *et al.*, arXiv:0903.2833.

[31] C. Lester *et al.*, arXiv:0903.3560v1.

[32] A. D. Christianson *et al.*, arXiv:0904.0767v1.